Theoretical Study of the Electrostatic and Steric Effects on the Spectroscopic Characteristics of the Metal-Ligand Unit of Heme Proteins. 2. C-O Vibrational Frequencies, ^{17}O Isotropic Chemical Shifts, and Nuclear Quadrupole Coupling Constants

Boris Kushkuley and Solomon S. Stavrov
Sackler Institute of Molecular Medicine, Sackler School of Medicine, Tel Aviv University, Ramat Aviv, Tel Aviv 69978, Israel

ABSTRACT The quantum chemical calculations, vibronic theory of activation, and London-Pople approach are used to study the dependence of the C-O vibrational frequency, ^{17}O isotropic chemical shift, and nuclear quadrupole coupling constant on the distortion of the porphyrin ring and geometry of the CO coordination, changes in the iron-carbon and iron-imidazole distances, magnitude of the iron displacement out of the porphyrin plane, and presence of the charged groups in the heme environment. It is shown that only the electrostatic interactions can cause the variation of all these parameters experimentally observed in different heme proteins, and the heme distortions could modulate this variation. The correlations between the theoretically calculated parameters are shown to be close to the experimentally observed ones. The study of the effect of the electric field of the distal histidine shows that the presence of the four C-O vibrational bands in the infrared absorption spectra of the carbon monoxide complexes of different myoglobins and hemoglobins can be caused by the different orientations of the different tautomeric forms of the distal histidine. The dependence of the ^{17}O isotropic chemical shift and nuclear quadrupole coupling constant on pH and the distal histidine substitution can be also explained from the same point of view.

INTRODUCTION

Many heme proteins (HPs) share the same prosthetic group, heme IX (Eichorn, 1973). Nevertheless, they perform a wide variety of functions, from reversible binding and storage of dioxygen by myoglobin (Mb) and hemoglobin (Hb) to cleavage of the O-O bond by cytochrome P450 (Ullrich, 1979) and electron transport by cytochrome *c*. That is why the mechanism of the control of the HP electronic structure and properties by the protein globule is one of the central problems of modern biochemistry and biophysics.

In our previous paper (paper 1, Kushkuley and Stavrov, 1996) we started a comprehensive theoretical analysis of the factors affecting the different spectroscopic characteristics of carbonylHPs (HP(CO)s); the active center of the latter was simulated by the iron porphyrin complex with imidazole (Im) and CO (Fe(P)(Im)CO) (Fig. 1). In that paper the quantum chemical calculations (QCCs) were used to study the effect of different heme distortions (Fig. 1 *b*), the homogeneous electric field, and the presence of the point Q_1 and Q_2 charges (Fig. 1 *c*) located on its CO side ("distal" charges) on the magnitudes of the orbital electron density transfers (OEDTs); the atomic bond indexes of the Fe-C and C-O chemical bonds; and the correlation between the corresponding vibrational frequencies (ν_{CO} and ν_{FeC}) in the HP(CO) active center. Then the vibronic theory of chemical activation by coordination (VTA) was applied to calculate the dependence of ν_{CO} on these perturbations.

VTA (Bersuker, 1978, 1984; Stavrov et al., 1993; Kushkuley and Stavrov, 1996) makes it possible to obtain such parameters of the coordinated ligand as its interatomic distances and force field constants without calculating its adiabatic potential, provided that the OEDTs to or from the ligand upon its coordination are known. The OEDTs along the valence orbitals can be reliably calculated by using semiempirical quantum chemical calculations. Therefore, the combined QCC-VTA approach can be used to quickly and reliably calculate (Stavrov et al., 1993, and paper 1) the stretching force field constants and vibrational frequencies of different diatomics (carbon monoxide and dioxygen) coordinated by HPs.

The comparison of the theoretical results of this combined QCC-VTA approach with the experimental data on ν_{CO} and ν_{FeC} of HP(CO)s and their model compounds showed that the distortions of the Fe(P)(Im)(CO) can explain by themselves neither the strong variation of ν_{CO}, nor its correlation with ν_{FeC} in the compounds under consideration, whereas the protein electric field could be responsible for the features of these vibrational frequencies.

This conclusion was consistent with the results of a number of recent experimental studies (Ricard et al., 1986; Kim et al., 1989; Kim and Ibers, 1991; Cameron et al., 1993; Quillin et al., 1993, 1995; Lian et al., 1993; Hu et al., 1994; Ivanov et al., 1994; Li et al., 1994; Ray et al., 1994; Springer et al., 1994; Tetreau et al., 1994; Lim et al., 1995), in which it was shown that the linear perpendicular coordination of CO in HP(CO)s is weakly distorted, if at all, and the wide variation of ν_{CO} in different HP(CO)s was as-

Received for publication 14 May 1996 and in final form 25 October 1996.
Address reprint requests to Dr. Solomon S. Stavrov, Sackler Institute of Molecular Medicine, Sackler School of Medicine, Tel Aviv University, Ramat Aviv POB 39040, Tel Aviv 69978, Israel. Tel.: 972-3-640-9859; Fax: 972-3-641-4245; E-mail: stavrov@post.tau.ac.il.

0006-3495/97/02/899/14 $2.00

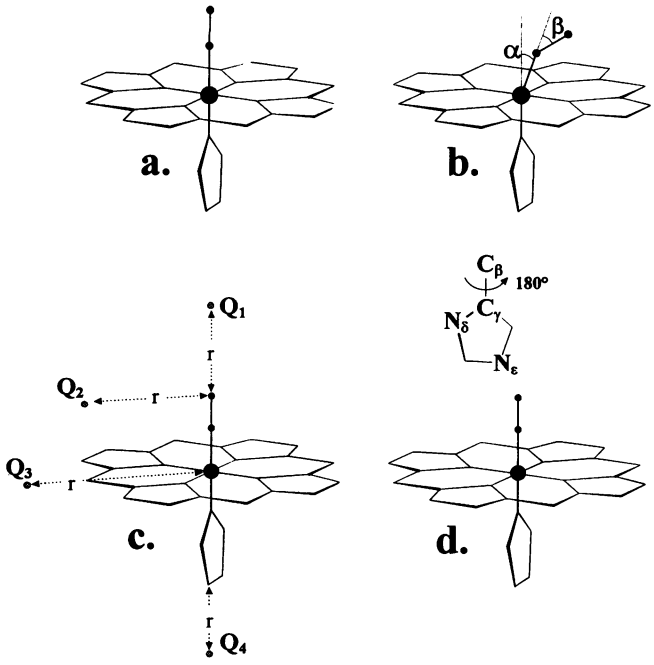

FIGURE 1 Schematic representation of the geometry of the complexes with linear perpendicular (*a*), bent and tilt (*b*), coordinated CO without and with (*c*) point charges Q_i, and in the presence of the distal histidine (*d*).

signed (Li and Spiro, 1988; Morikis et al., 1989; Augspurger et al., 1991; Oldfield et al., 1991; Park et al., 1991; Brantley et al., 1993; Lian et al., 1993; Cameron et al., 1993; Sakan et al., 1993; Hu et al., 1994; Ivanov et al., 1994; Li et al., 1994; Ray et al., 1994; Springer et al., 1994; Decatur and Boxer, 1995) to the effect of the protein electric field (Geissinger et al., 1995).

For example, Oldfield et al. (1991) presented a molecular model of the four major "conformational substates" observed by infrared spectroscopy in Mb(CO)s and Hb(CO)s, in terms of an electrical perturbation of ν_{CO} due to the possibility of $H^{\epsilon} \leftrightarrow H^{\delta}$ tautomerism, and 180° C_{β}-C_{γ} ring flips, of distal histidine residue (see Fig. 1 *d*). This assumption was supported by the molecular dynamics calculations of Jewsbury and Kitagawa (1994, 1995), who showed that the distal histidine (His) dynamics can be described as a motion along four qualitatively different trajectories, each of which was assumed to correspond to the conformational substate.

The results of the electron spin echo envelope modulation spectroscopy of different oxyCo(II)-substituted distal histidine myoglobin mutants (Lee et al., 1994) also supported the conclusion about the effect of the distal histidine electric field on the heme properties.

The inference about the linear perpendicular CO coordination was questioned by Jewsbury et al. (1995), who determined, by using ab initio quantum chemical calculations, that the linear perpendicular CO coordination geometry must be strongly distorted (30–60°) upon the relatively weak distortion of the proximal histidine coordination in Fe(P)(Im)(CO). This conclusion, however, is not supported by the precise x-ray studies of the model complexes with hindered and nonhindered imidazoles, where almost the same hardly distorted coordination geometry of CO was observed (Kim et al., 1989; Kim and Ibers, 1991; Ricard et al., 1986; Tetreau et al., 1994), or by other quantum chemical calculations (Ghosh and Bocian, 1996).

Recently (Park et al., 1991) ^{17}O nuclear magnetic resonance spectroscopy (NMR) was applied to study the effect of protein on electron density transfer (EDT) to the coordinated CO in HP(CO)s. In this paper the correlations between ν_{CO}, ν_{FeC}, and ^{17}O isotropic chemical shifts (δ) and the nuclear quadrupole coupling constant (Γ) of the coordinated CO were found and qualitatively interpreted to be a result of the interaction with the electric field of different amino acids.

Despite the intensive experimental investigation of the effect of the protein environment on the properties of the FeCO unit, quantum chemical studies were made of the electric field effects on the NMR characteristics of only the free carbon monoxide molecules (Augspurger et al., 1991). These studies showed that polarization of this molecule must itself lead to the pronounced dependence of its isotropic chemical shifts on the field.

In this work we 1) continue to investigate the effect of different charged groups on the heme OEDT and ν_{CO}; 2) perform a theoretical investigation of the effect of geometry distortions of the HP active center on δ and Γ; 3) investigate the effect of electrostatic interactions on these NMR parameters; and 4) calculate the effect of the electric field of the distal histidine on all the considered spectroscopic characteristics of the coordinated CO in Mb(CO).

In particular, the following general questions will be answered:

1. To what extent can δ and Γ be affected by different distortions of the active center?
2. To what extent can the protein charged groups affect ν_{CO}, δ, and Γ?
3. How can the distal histidine affect these parameters?

To realize this plan, the QCCs (Ridley and Zerner, 1973; Bacon and Zerner, 1979; Zerner et al., 1980; Anderson et al., 1986; Edwards et al., 1986), VTA (Bersuker, 1978, 1984; Stavrov et al., 1993; Kushkuley and Stavrov, 1996) and the theories of isotropic chemical shifts (London, 1937; Pople, 1962) and nuclear quadrupole splitting (Lucken, 1969; Poole and Farach, 1972; Semin et al., 1975) are used. These techniques make it possible to study theoretically the dependence of the parameters under consideration on the distortion of the CO coordination geometry, change in the iron-carbon and iron-imidazole distances, displacement of the iron out of the porphyrin plane, ruffling and doming of the porphyrin ring, a homogeneous electric field, and point charges located in the heme vicinity.

For all of the QCCs, the active center of HP(CO) is simulated by the Fe(P)(Im)(CO) complex, whereas the charged or polar amino acids are simulated by point charges or a homogeneous electric field.

METHODS

Isotropic chemical shifts

The London-Pople approach (London, 1937; Pople, 1962) was used for the calculation of δ. Below are the main formulae of this approach.

In NMR experiments nuclei with magnetic moments are effectively used as probes to measure the actual magnetic field (H_{loc}) at the nucleus.

$$H_{loc} = (1 - \sigma)H, \tag{1}$$

where H is the applied magnetic field strength and σ is the total shielding constant. Its value for a particular nucleus can be approximated by a sum of three terms:

$$\sigma = \sigma_d + \sigma_p + \sigma'. \tag{2}$$

The term σ' represents the effect of the electronic circulation on all other atoms and any interatomic ring currents that cannot be localized. The diamagnetic contribution σ_d is the Lamb term for the atom being considered and corresponds to the uniform circulation of the atomic electrons as if they were free. The paramagnetic term σ_p is a local correction due to the molecular environment and involves the mixing of ground and excited electronic states by the applied magnetic field. Hereafter only the latter two terms (σ_d and σ_p) are taken into consideration, inasmuch as the contribution of σ' is much smaller (Karplus and Pople, 1963). For the estimation of their magnitude it is convenient to use molecular orbital–linear combination of atomic orbitals (MO-LCAO) theory. Each MO Ψ_i is expressed as a linear combination of valence-shell atomic orbitals ϕ_μ:

$$\Psi_i = \sum_\mu c_{i\mu}\phi_\mu. \tag{3}$$

If the molecule is placed in a magnetic field, the LCAO coefficients, $c_{i\mu}$, are changed slightly and the perturbation theory can be used. It was obtained (Pople, 1962) using the perturbation theory, London approximation (London, 1937), and averaging over different directions of the magnetic field (this procedure is necessary to study the complexes in a solution or powder):

$$\sigma_d^A = \frac{e^2}{3mc^2}\langle r^{-1}\rangle^A q^A, \tag{4}$$

$$\sigma_p^A = -\frac{2e^2\hbar^2}{m^2c^2}\langle r^{-3}\rangle^A \Theta^A, \tag{5}$$

$$\Theta^A = \frac{1}{3}\sum_{\alpha=x,y,z}\sum_i^{occ}\sum_j^{unocc}(\epsilon_j - \epsilon_i)^{-1} \times \sum_{\mu<\nu}^{A}\sum_B\sum_{\lambda<\rho}^{B}(c_{i\mu}c_{j\nu} - c_{i\nu}c_{j\mu})(c_{i\lambda}c_{j\rho} - c_{i\rho}c_{j\lambda})(l_\alpha)_{\mu\nu}(l_\alpha)_{\lambda\rho}, \tag{6}$$

where q^A is the electronic density on atom A; ϵ_i is the energy of the ith molecular orbital; Σ_i^{occ} (Σ_i^{unocc}) is a sum over occupied (unoccupied) MOs; $\Sigma_{\mu<\nu}^{A}$ ($\Sigma_{\lambda<\rho}^{B}$) is a sum over all atomic orbitals μ and ν of atom A (λ and ρ of atom B), only if $\mu < \nu$ ($\lambda < \rho$); Σ_B is a sum over all atoms in the molecule; $(l_\alpha)_{\mu\nu}$ is a corresponding matrix element of the α component of the angular momentum vector $\mathbf{l} = \mathbf{r} \times \nabla$. For the calculation of δ, the diagonal matrix elements of the inverse distance of electron i from the nucleus (r^{-1} and r^{-3} operators) are calculated by using Slater 2s and 2p atomic orbitals:

$$\langle r^{-3}\rangle^A = \frac{1}{24}(Z^A/a_0)^3, \tag{7}$$

and

$$\langle r^{-1}\rangle^A = \frac{1}{4}(Z^A/a_0), \tag{8}$$

where a_0 is the Bohr radius, and the oxygen effective nuclear charge $Z^O = 7.95$ e^- is chosen according to Slater's rules (Slater, 1930). $(l_\alpha)_{\mu\nu}$ values are taken from Jameson and Gutowsky (1964) and Buchner and Schenk (1982).

It was shown earlier (see, for example, Jameson, 1994) that semiempirical methods cannot give the appropriate absolute values of isotropic chemical shifts. Therefore we will discuss below the calculated and experimentally observed changes of δ,

$$\Delta\delta = \Delta(-\sigma). \tag{9}$$

Nuclear quadrupole coupling constant

The quadrupole interaction operator (Lucken, 1969; Poole and Farach, 1972; Semin et al., 1975) arises from the interaction between the nuclear spin I and the quadrupole energy tensor:

$$\overleftrightarrow{Q} = \begin{pmatrix} Q_{xx} & Q_{xy} & Q_{xz} \\ Q_{yx} & Q_{yy} & Q_{yz} \\ Q_{zx} & Q_{zy} & Q_{zz} \end{pmatrix}, \tag{10}$$

$$Q_{ij} = \frac{eQ}{2I(2I-1)}V_{ij}, \tag{11}$$

Q is the scalar quadrupole moment and V_{ij} is the electric field gradient. For the calculation of the experimentally observed value of the electric field gradient, the matrix elements of the $\hat{V}_{ij}$ operator on Slater's multielectron determinants, Φ, must be taken:

$$V_{ij} = \langle\Phi|\hat{V}_{ij}|\Phi\rangle = \sum_{k,l}^{occ.MO}\langle\Psi_k|\hat{V}_{ij}|\Psi_l\rangle = \sum_{k,l}^{occ.MO}\sum_{\alpha,\beta}^{AO} c_{k\alpha}c_{l\beta}\langle\phi_\alpha|\hat{V}_{ij}|\phi_\beta\rangle. \tag{12}$$

The quadrupole energy tensor has a principal coordinate system $x'y'z'$ in which it is diagonal. Using the principal values $Q_{x'x'}$, $Q_{y'y'}$, and $Q_{z'z'}$, we can write down the expression for the oxygen Γ, spin 3/2 (Poole and Farach, 1972):

$$\Gamma = Q_{z'z'}\sqrt{1 + \frac{\eta^2}{3}}, \tag{13}$$

where η is the asymmetry parameter:

$$\eta = \left|\frac{Q_{x'x'} - Q_{y'y'}}{Q_{z'z'}}\right|, \tag{14}$$

and $|Q_{x'x'}| \le |Q_{y'y'}| \le |Q_{z'z'}|$.

As in the case of the calculations of δ, the semiempirical QCCs used in this work make it possible to calculate only the changes in $Q_{i'i'}$ upon alteration of the structure of the complex and not their absolute values. As a result, only the relative changes in Γ can be calculated with this approach. It follows from this conclusion that the absolute value of η also cannot be calculated by using this approach because of the presence of the absolute $Q_{z'z'}$ value in the denominator of Eq. 14. Therefore, to characterize the dependence of the rhombic x'-y' asymmetry of the distribution of the electron cloud around the oxygen on the complex structure, the magnitude of $|Q_{x'x'} - Q_{y'y'}|$ is used.

Quantum chemical calculations of electronic structure

The intermediate neglect of differential overlap (INDO) version of the MO-LCAO approach (Ridley and Zerner, 1973; Bacon and Zerner, 1979; Zerner et al., 1980; Anderson et al., 1986; Edwards et al., 1986) is used for quantum chemical study of the electronic structure of the closed-shell Fe(P)(Im)(CO) complex (156 electrons), OEDTs, and their dependence on the complex distortions and electrostatic interactions. This type of approach is based on the self-consistent solution of the Hartree-Fock equation, with the inclusion of all the one-center exchange terms necessary for rotational invariance and accurate spectroscopic predictions, as well as an accurate description of integrals involving 3d atomic orbitals. INDO is the technique in which one-center core integrals are obtained just from ionization potentials. In this work the spin-restricted Hartree-Fock method is used and the calculations were performed using a basis set of single Slater-type orbitals and spectroscopic Mataga-Nishimoto parameterization (Ridley and Zerner, 1973; Bacon and Zerner, 1979; Zerner et al., 1980). For quantum chemical calculations by this method we used the ZINDO program kindly supplied by Dr. M. Zerner (Department of Chemistry, University of Florida), which was succesfully used earlier to study iron-porphyrin complexes (Edwards et al., 1986, 1988; Loew, 1983; Du et al., 1991; Du and Loew, 1992, 1995)

In these calculations the same basic structure of Fe(P)(Im)(CO) is used as in paper 1 (Kushkuley and Stavrov, 1996). Because the geometry of the porphyrin ring of different model compounds in different crystals is differently distorted from its high symmetry configuration by the crystal environment, in our basic structure the porphin ring is assumed to have a high-symmetry D_{4h} structure, which was obtained earlier from the analysis of a number of the porphyrin compounds (see table 6 of Eaton et al., 1978). The structure of the imidazole is also taken from the same paper, and the C-O distance equals that in the free diatomic molecule. The F-CO and Fe-Im distances are taken to be 1.745 Å and 2.06 Å, respectively. This basic structure is used as a starting point for study of the effects of different hypothetic complex distortions and model point charges on the complex properties.

For the QCCs of the effect of the distal histidine electric field in Mb(CO), the structures of the Fe(P)(Im)(CO) complex, distal histidine, and their relative positions are taken from the x-ray diffraction study of wild-type sperm whale (SW) Mb(CO) (PDB entry: 2MGK; Quillin et al., 1993); all of the porphyrin side chains are substituted for hydrogen atoms.

Vibronic theory of chemical activation by coordination

VTA is described in detail elsewhere (Bersuker, 1978, 1984; Stavrov et al., 1993; Kushkuley and Stavrov, 1996). Its main idea is to make a bridge between the widespread MO description of the electronic structure on the one hand and the coupling of electronic states with the nuclear configuration described by the vibronic coupling theory on the other.

In particular, it was shown by using VTA that the following expression for the force field constant of the normal vibration Q in the γth electronic state can be written:

$$K^{\gamma} = \sum_{i} q_i^{\gamma} k_i, \qquad (15)$$

where q^{γ}_i is the population of the ith orbital in the γth electronic state, and k_i is the second-order orbital vibronic constant. It follows from this expression that the dependence of the force-field constant K^{γ} on the structure of any compound in any γ electronic state is mainly controlled by the MO populations q^{γ}_i or, in other words, by OEDTs to or from MOs under consideration.

RESULTS

The dependence of OEDTs, ν_{CO}, and Fe-C-O atomic bond indexes on the presence of the equatorial and proximal point charges

Point charges of $Q = \pm 1.0\, e^-$ were located in the porphyrin plane at r = 8.0 Å, 9.0 Å, 10.0 Å, and 12.0 Å from the iron (Fig. 1 *c*, Q_3) and on the imidazole side of Fe(P)(Im)(CO) complex along the Fe-N_{Im} bond at the distances r = 2.5 Å, 3.0 Å, 4.0 Å, 5.0 Å, and 7.0 Å from the hydrogen of the distal nitrogen of the proximal imidazole (Fig. 1 *c*, Q_4). For simplicity, from here on the former Q_3 and latter Q_4 charges are referred to as the "equatorial" and "proximal" charges.

The results of QCCs show that the presence of the proximal charge significantly affects the OEDTs from the 5σ and to the $2\pi^*$ MOs of the coordinated CO (Fig. 2, *a* and *b*). It follows from Fig. 3, *a* and *b*, that these OEDTs significantly affect the Fe-C and C-O atomic bond indexes (B_{FeC} and B_{CO})—the larger the index, the stronger the corresponding bond. VTA shows that these OEDT changes essentially affect ν_{CO} (Fig. 4 *a*).

The effect of the equatorial charges is weaker than that of the proximal ones, but is still notable (see Figs. 2 *c*, 2 *d*, 3 *a*, 3 *b*, and 4 *b*).

Effect of the Fe(P)(Im)(CO) distortions on the ^{17}O NMR parameters

The effect of the change in the Fe-CO distance (R_{FeC}) was studied by using QCCs of the electronic structure of the Fe(P)(Im)(CO) complexes with linearly perpendicular coordinated CO located at different distances from the iron (Fig. 1 *a*). The magnitude of the latter was varied in the interval from 1.73 to 1.77 Å, which was determined from the x-ray structure data on the model compounds (Ricard et al., 1986; Kim et al., 1989; Kim and Ibers, 1991; Tetreau et

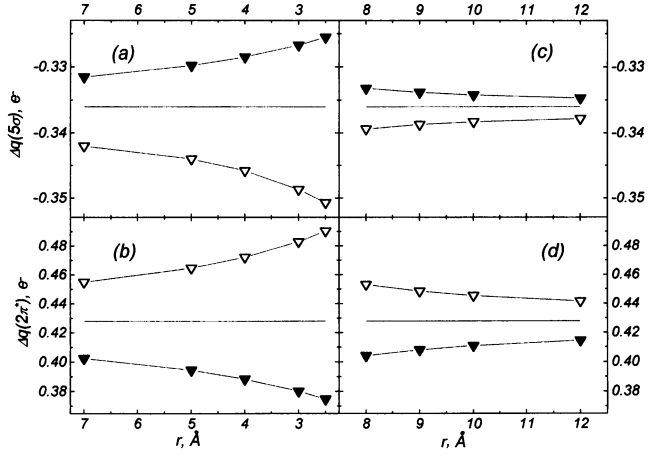

FIGURE 2 Dependence of the σ donation (*a* and *c*) and back-bonding (*b* and *d*) on the location and magnitude of the proximal Q_4 (*a* and *b*) and equatorial Q_3 (*c* and *d*) point charges. ▲, $+1\, e^-$; △, $-1\, e^-$; ——, no charge.

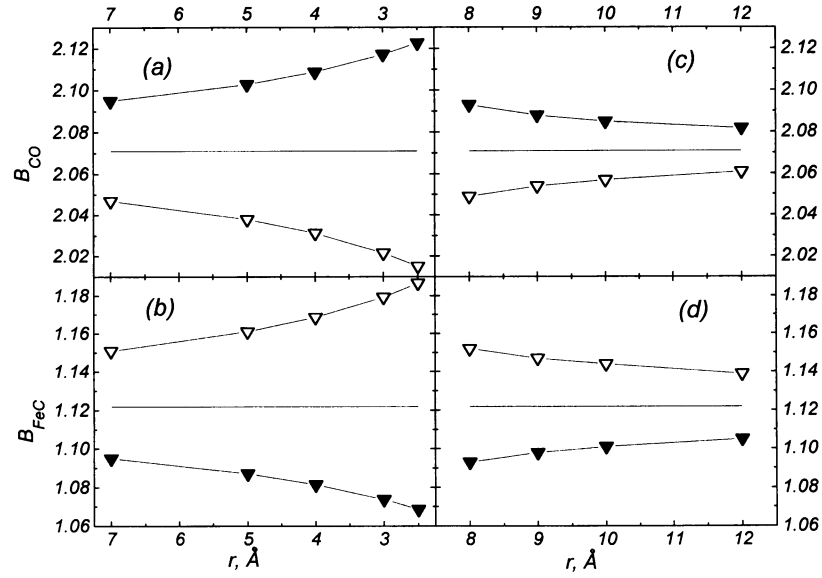

FIGURE 3 Dependence of the C-O (*a* and *c*) and Fe-C (*b* and *d*) atomic bond indexes on the location and magnitude of the proximal Q_4 (*a* and *b*) and equatorial Q_3 (*c* and *d*) point charges. Notations for different charge magnitudes are the same as in Fig. 2.

al., 1994). The results of calculations (Table 1) show that the R_{FeC} change notably affects both δ and Γ.

The effect of the displacement of the iron out of the porphyrin plane was studied by QCCs of the complexes with the axial nuclear subsystem CO-Fe-Im displaced 0.1 Å as a whole in both directions with respect to the porphyrin plane. These distortions are larger than the experimentally observed ones (Ricard et al., 1986; Kim et al., 1989; Kim and Ibers, 1991; Tetreau et al., 1994) and hardly change both Γ and δ.

The changes of the iron-imidazole distance (R_{FeN}) were simulated by varying R_{FeN} from 2.04 to 2.08 Å (Ricard et al., 1986; Kim et al., 1989; Kim and Ibers, 1991; Tetreau et al., 1994). QCCs of all of these structures show that this bond alteration hardly affects both δ and Γ.

Electronic structures of the different complexes with the S_4 ruffled and domed porphyrin rings (see paper 1 (Kushkuley and Stavrov, 1996) for a comprehensive description of the deformations studied) on Γ and δ were studied. The results show that the ruffling deformations of the porphyrin ring nuclear configuration hardly change Γ and δ. The effect of the porphyrin doming is presented in Table 1.

To investigate the effects of the CO distortion on Γ and δ, the Fe(P)(Im) complexes with bend, tilt, and bend-tilt coordinated CO (Fig. 1 *b*) were studied. The calculated δ for different values of α and β angles are presented in Table 1. The results show that the tilt and especially the simultaneous tilt and bent of the Fe-C-O unit can significantly affect both Γ and δ.

The changes in R_{FeN} and R_{FeC} and the various heme distortions do not lead to any pronounced change in the rhombic asymmetry parameter $|Q_{x'x'} - Q_{y'y'}|$. However, any studied distortion in the CO coordination geometry strongly increases the rhombic asymmetry of the electron density distribution on the oxygen (Table 1).

The effect of the point charges and homogeneous electric field on Γ and δ

The effect of different point charges (Q_i) on the NMR parameters of the Fe(P)(Im)(CO) complex with linearly coordinated CO (Fig. 1 *c*) was studied by using QCCs of its electronic structure in the presence of $\pm 1.0\ e^-$ distal charges located at distances of r = 2.5, 3.0, 4.0, 5.0, and 7.0 Å from the CO oxygen in the direction perpendicular (Fig. 1 *c*, Q_1) and parallel to the porphyrin plane (Fig. 1 *c*, Q_2), and in the presence of the equatorial Q_3 and proximal Q_4 charges (Fig. 1 *c*).

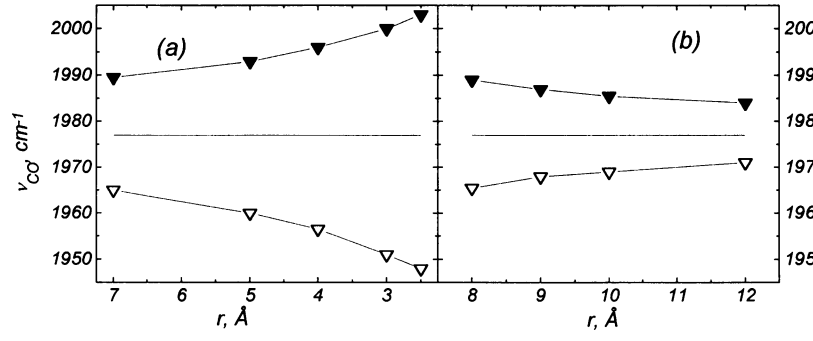

FIGURE 4 Dependence of ν_{CO} on the location and magnitude of the proximal Q_4 (*a*) and equatorial Q_3 (*b*) point charges. Notations for different charge magnitudes are the same as in Fig. 2.

TABLE 1 The changes in δ and Γ caused by the different heme distortions

	$\Delta\delta$ (ppm)	$\Delta\Gamma$ (MHz)	$\lvert Q_{y'y'} - Q_{z'z'}\rvert$ (MHz)
FeCO tilt (α = 15°, β = 0)	−1.98	−0.21	0.99
FeCO bend (α = 0, β = 45°)	0.04	0.03	0.51
FeCO tilt and bend (α = 13°, β = 45°)	−4.88	−0.28	1.09
Porphyrin doming	−2.08	0.04	0.01
$R_{Fe\text{-}C}$ = 1.77 Å	0.43	0.11	0.01
$R_{Fe\text{-}C}$ = 1.73 Å	−0.17	−0.04	0.01

It was obtained that all of the charges in the heme vicinity strongly affect δ and Γ (Fig. 5). Nevertheless, there is no notable effect of the point charges on the rhombic asymmetry of the diagonalized quadrupole coupling tensor.

The dependence of δ and Γ on a homogeneous electric field of the magnitude −0.01 to 0.01 au (1 au = 5.14225×10^9 V/cm), oriented perpendicular and parallel to the porphyrin plane, was also studied. The results show that the field oriented parallel to the porphyrin plane hardly affects any of these values. The perpendicular field of 0.01 (− 0.01) au changes Γ by 0.34 (−0.35) MHz and δ by 9 (− 10) ppm; the dependence of these parameters on the field magnitude is almost linear.

Neither the perpendicular nor the parallel homogeneous electric field, at the considered magnitude, leads to notable rhombic asymmetry of the electron density distribution on the CO oxygen.

Effect of the distal histidine electric field on the spectroscopic parameters under consideration

For the QCCs the distal histidine was simulated by the point charges located at the places of the histidine imidazole atoms (Fig. 1 *d*), the charge magnitudes being taken from the histidine electric field simulation (Chipot et al., 1992).

The effect was studied of the electric field of the four different conformational substates (His^{δ}, His^{ϵ}, $His^{\delta,180}$ and $His^{\epsilon,180}$) (Oldfield et al., 1991) of the neutral distal histidine. The two former substates correspond to the tautomers of neutral imidazole with a protonated proximal N_{ϵ} (His^{ϵ}) or distal N_{δ} (His^{δ}) nitrogen. The two latter substates correspond to these two imidazole tautomers rotated by 180° about the C_{β}-C_{γ} bond between the imidazole and the rest of the distal histidine residue (Fig. 1 *d*).

The effect of the electric field of the distal histidine cation with protonated N_{ϵ} and N_{δ} (His^{+}) was also studied.

In these calculations the experimentally determined atomic coordinates of the Fe(P)(Im) part of the active center were used. Because the latest spectroscopic and x-ray studies show that CO is coordinated approximately perpendicular to the porphyrin plane (Fig. 1 *a*), in our calculations it was placed along the Fe-N_{Im} line at distances R_{FeC} = 1.90 Å and 1.75 Å, which equal the x-ray values in Mb(CO) (Quillin et al., 1993) and model compounds (Ricard et al., 1986; Kim et al., 1989; Kim and Ibers, 1991; Tetreau et al., 1994). Usage of these two values leads to the values of ν_{CO} = 2046.2 and 1978.5 cm^{-1}, respectively. The former is unrealistically high, being much higher than the experimentally observed ones in Mb(CO) and model compounds.

Therefore, it was assumed in our calculations that R_{FeC} = 1.75 Å in both Mb(CO) and model compounds. The results of the calculations of the changes in ν_{CO}, δ, and Γ caused by the electric field of His^{δ}, His^{ϵ}, $His^{\delta,180}$, $His^{\epsilon,180}$ and His^{+} are presented in Table 2.

DISCUSSION

Effect of the proximal and equatorial charges on OEDTs, ν_{CO}, B_{CO}, and B_{FeC}

It follows from the results that the proximal and equatorial point charges essentially affect OEDTs, ν_{CO}, and B_{FeC} and B_{CO} (Figs. 2–4). Like the distal charges (Kushkuley and Stavrov, 1996), the proximal charges significantly change π back-bonding, σ donation being much more weakly affected. For example, a charge of 1 e^{-} located 3.0 Å from the edge of proximal imidazole (Fig. 1 *c*, Q_4) changes the population of $2\pi^*$ MO by 0.05 e^{-} and that of 5σ MO by less then 0.01 e^{-}. These OEDTs have to affect the strengths

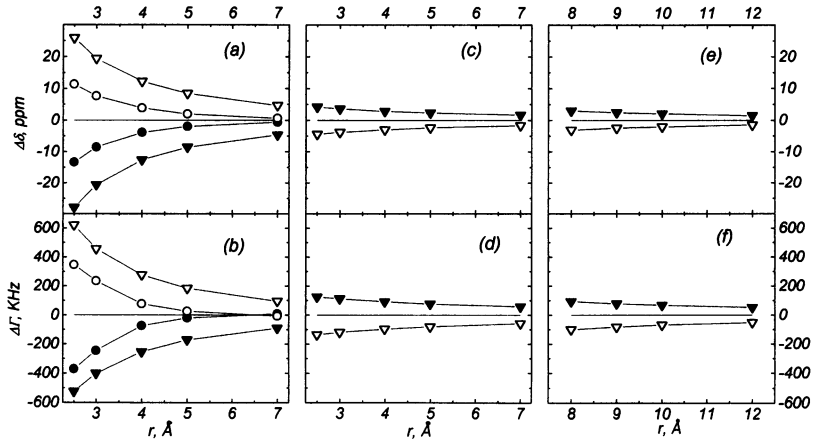

FIGURE 5 Dependence of $\Delta\delta$ (*a*, *c*, and *e*) and $\Delta\Gamma$ (*b*, *d*, and *f*) on the location and magnitude of the distal Q_1 and Q_2 (*a* and *b*), proximal Q_4 (*c* and *d*), and equatorial Q_3 (*e* and *f*) point charges. Notations for different charge magnitudes are the same as in Fig. 2, except for *a* and *b*, where the solid (open) triangles and circles correspond to the distal +1 e^{-} (−1 e^{-}) Q_1 and Q_2 point charges, respectively

TABLE 2 The calculated changes in B_{CO}, B_{FeC}, ν_{CO}, δ, and Γ caused by the electric field of the distal histidine

	ΔB_{CO}	ΔB_{FeC}	$\Delta\nu_{CO}$ (cm^{-1})	$\Delta\delta$ (ppm)	$\Delta\Gamma$ (MHz)
His^{δ}	0.05	−0.03	15.6	3.1	0.09
$His^{\epsilon,180}$	0.03	0	3.5	2.3	0.05
$His^{\delta,180}$	−0.01	0.02	−6.9	−1.8	−0.05
His^{ϵ}	−0.02	0.03	−13.6	−2.2	−0.07
His^{+}	−0.06	0.05	−30.1	−7.4	−0.19

of the Fe-C and C-O bonds. Indeed, the charge under consideration changes the corresponding bond indexes by 0.05 in the opposite direction. In comparing these results with those of paper 1, one should note that despite the fact that the Q-CO distance in the case of proximal charges is much larger than that in the case of the distal charges, the effects of the proximal and distal charges on $\Delta q(2\pi^*)$ are akin. This effect is a direct manifestation of the large polarizability of the π subsystem of the Im-Fe-CO unit (Park et al., 1991; Li and Spiro, 1988; Lee et al., 1992, 1993, 1994, 1995).

Equatorial charges (Fig. 1 *c*, Q_3) lead to a weaker OEDT along both the π and σ subsystems (0.015 e^- and 0.002 e^-, respectively, for the unit charge 9 Å from the iron). However, even these weak OEDTs also cause a notable change in B_{FeC} and B_{CO} (0.02 for the charge under consideration).

As in the case of the distal Q_1 charges, the correlation between B_{FeC} and B_{CO} (Fig. 6) is almost linear for each of the charge locations with the slopes $\alpha_B \approx -1.1$ and -1.4 for the equatorial and proximal charges, respectively. In paper 1 $\alpha_\nu = \Delta\nu_{FeC}/\Delta\nu_{CO}$ was shown to equal $\alpha_\nu \approx \frac{1}{2}\alpha_B$. Therefore, it follows from our calculations that different equatorial and proximal charges are expected to notably affect both ν_{FeC} and ν_{CO}, α_ν being equal to -0.55 and -0.7, respectively. These values are very close to the coefficient of the experimentally obtained $\alpha_\nu \approx -0.75$ (Li and Spiro, 1988; Oldfield et al., 1991; Ray et al., 1994). This fact shows that, in principle, the experimental correlation between ν_{CO} and ν_{FeC} can be caused by the change of position of some protein or/and heme charged groups located in the proximal or equatorial parts of the heme pocket.

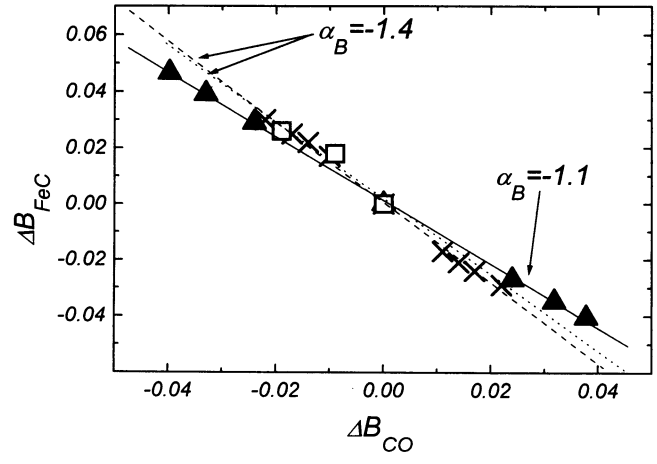

FIGURE 6 The correlation between the calculated changes in B_{FeC} and B_{CO} caused by the appearance of the different proximal Q_4 (×) and equatorial Q_3 (▲) point charges and changes of the tautomeric form and orientation of the distal histidine (□).

The effect of the proximal and equatorial charges on back-bonding is manifested in the essential dependence of ν_{CO} on their magnitude and location (Fig. 4). For example, the location of the negative unit charge 3 Å from the proximal Im edge (more than 9 Å from the CO ligand) decreases ν_{CO} by 20 cm^{-1}, whereas the equatorial charge of the same magnitude located 9 Å from the iron lowers ν_{CO} by 8 cm^{-1}.

Effect of the Fe(P)(Im)(CO) geometry distortions on the ^{17}O NMR parameters

It follows from our calculations that the porphyrin ring deformation, the iron out-of-plane displacement, CO bending, and the alteration of R_{FeN} hardly affect δ and Γ. A decrease in R_{FeC} by 0.01 Å decreases these parameters by approximately 0.15 ppm and 0.04 MHz, respectively (Table 1), which are considerably smaller than the corresponding variations in the heme proteins and their models (about 10 ppm and 0.5 MHz). These results allow us to conclude that these distortions by themselves cannot explain the experimentally observed wide variation in δ and Γ and their correlation with $\nu_{C\text{-}O}$ (Park et al., 1991).

The tilt ($\alpha = 15°$) and, in particular, the combined tilt and bend ($\alpha = 15°$, $\beta = 45°$) of the Fe-CO bond notably change δ (−2.0 ppm and −4.9 ppm, respectively) and Γ (−0.21 MHz and −0.28 MHz, respectively). These results show that the tilt or combined tilt and bend of CO can, in principle, contribute to the distribution of the experimentally observed δ and Γ values. However, as it was mentioned in the Introduction, the latest x-ray and spectroscopic experimental data show that the linear perpendicular coordination of CO is hardly distorted (if at all) in HP(CO)s and their models.

It follows from the data on $|Q_{x'x'} - Q_{y'y'}|$ that the distortions of the porphyrin plane and changes in R_{FeN} and R_{FeC} hardly affect the rhombic asymmetry of the electron density distribution around the oxygen atom. However, the bend and tilt of CO lead to its nonaxial coordination. Therefore, these distortions, if they take place, are expected to make the populations of the p_x and p_y oxygen orbitals very different and, consequently, strongly increase the Γ rhombicity. This qualitative conclusion is in full agreement with the results of our calculations (see Table 1).

Effect of the external electric field on the ^{17}O NMR parameters

The OEDTs caused by the point charges and external electric field are also supposed to affect the ^{17}O NMR parameters. Indeed, our calculations show that the distal charges

considerably affect δ and Γ. For example, a positive Q_1 unit charge located 3 Å from the oxygen (Fig. 1 *c*) decreases δ and Γ by approximately 21 ppm and 0.4 MHz, respectively, although the distal Q_2, equatorial Q_3, and proximal Q_4 point charges (Fig. 1 *c*) affect δ and Γ much more weakly (Fig. 5).

To understand this result, the parameter of the Fe(P)(Im)(CO) electronic structure that mainly controls δ must be elucidated. Because δ is a measure of the electron cloud contribution to the actual magnetic field on the oxygen nucleus, it is expected to correlate with the electron density on the oxygen. To test this qualitative conclusion, all of the changes in the δ value calculated in this work were plotted against the corresponding changes in the Mulliken electron density on the oxygen (q) (Fig. 7). It follows from this figure that there is an approximately linear correlation between $\Delta\delta$ and Δq, with the slope of the line $\Delta\delta/\Delta q = -141$ ppm/e^-. This result supports the qualitative conclusion and shows that δ can be used as a measure of the net electron density (sum of σ and π) on the oxygen atom of the coordinated CO.

Consequently, the large changes in δ must be caused by the charges, which strongly affect electron density on the oxygen. The latter is controlled by the difference between the electrostatic potential on the oxygen and other parts of the complex. The greatest difference is produced by the distal Q_1 charges (see paper 1 for discussion). Therefore, δ is very strongly affected by the Q_1 charges, the effect of the distal Q_2 charges is approximately 40% weaker, and the effects of the proximal and equatorial charges are even weaker (Fig. 5).

To qualitatively understand the effect of the point charges on Γ, note that its change in the external electric field stems mainly from the redistribution of the valence electron density. It is simple to determine from Eq. 12 that in the axially symmetric molecular system this change is proportional to the change in

$$N = N(p_z) - 1/2[N(p_y) + N(p_x)], \qquad (16)$$

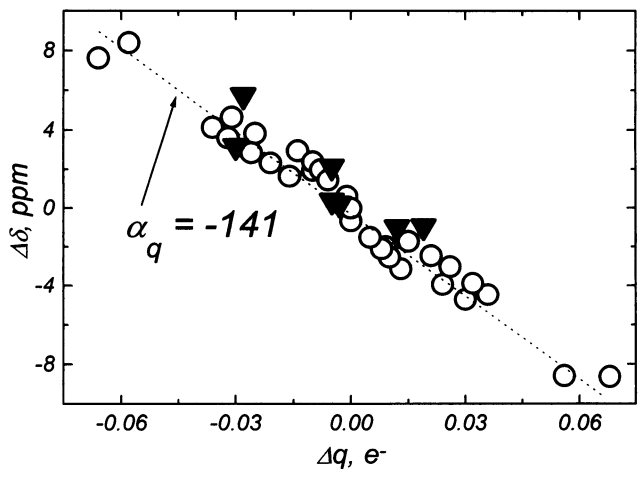

FIGURE 7 Correlation between the calculated values of $\Delta\delta$ and Δq for all of the considered distortions (▲) and point charges (○).

where $N(p_i)$ is a population of the p_i oxygen orbital, and the z axis coincides with the axis of symmetry. Because Γ is positive (Park et al., 1991), any decrease (increase) in N must decrease (increase) Γ.

Let us now consider the effect of the distal positive Q_1 charge. It was shown in paper 1 that this charge affects the electron density distribution in the complex under consideration, mainly by increasing the back-bonding. Therefore it increases the population of the p_x and p_y oxygen orbitals; the population of the p_z orbital is changed less dramatically. Consequently, the reduction of Γ is expected in this case; this qualitative conclusion is in full agreement with the results of our calculations (Fig. 5).

The results of our calculations show that there is no significant effect on δ and Γ of a homogeneous electric field oriented parallel to the porphyrin plane. To understand this result, it is necessary to take into account that such a field on the one hand does not produce any notable difference in electrostatic potentials between O and other parts of the complex. On the other hand, EDT in the porphyrin does not affect the axial subsystem, because the last one is oriented perpendicular to the electric field and is located in the porphyrin center.

A homogeneous electric field perpendicular to the porphyrin plane significantly affects EDT along the Im-Fe-CO unit, changing electron density on the oxygen and affecting both δ and Γ.

Correlation between δ, Γ, and ν_{CO}

The combined QCC-VTA studies started in paper 1 and continued in this paper allowed us to directly calculate the effect of different point charges on ν_{CO}. The calculation of the effect of the same charges on δ and Γ allows us to compare the theoretically and experimentally obtained correlations between these three spectroscopic characteristics of HP(CO)s and their models.

To qualitatively understand the character of the correlations between these three parameters, let us consider the effect of the negative proximal Q_4 charge. This charge increases EDT to CO and, consequently, q. The former increase was shown in paper 1 to decrease ν_{CO}, whereas the latter decreases both δ and Γ (see Fig. 7). Therefore, the point charges located in the vicinity of the heme are expected to change ν_{CO}, δ, and Γ in the same direction.

The calculated changes in δ are plotted in Fig. 8 *b* against the corresponding changes in ν_{CO} for each of the considered cases. It follows from this figure that, indeed, δ and ν_{CO} are changed by the homogeneous electric field and the Q_1, Q_3, and Q_4 point charges in the same direction, and the correlation between them is close to a straight line.

It follows from Fig. 8 *b* that the line slopes (α_δ) are different in different cases:

$$\Delta\delta = (0.15 \div 0.47)\Delta\nu_{co}\ \text{ppm/cm}^{-1}, \qquad (17)$$

where the 0.15 and 0.47 values correspond to the proximal (Q_4) and distal (Q_1) point charges. To qualitatively under-

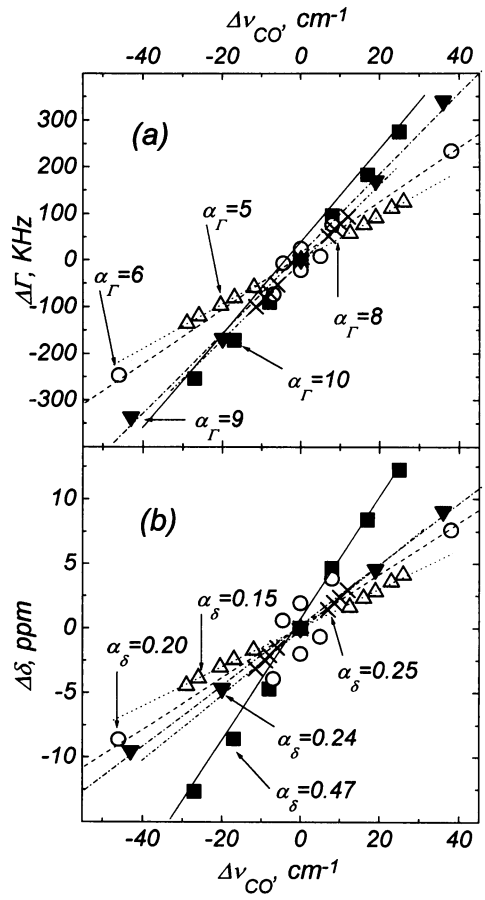

FIGURE 8 The correlation between the calculated values of $\Delta\Gamma$ and $\Delta\nu_{CO}$ (*a*), and $\Delta\delta$ and $\Delta\nu_{CO}$ (*b*) caused by the distal Q_1 (■) and Q_2 (○), equatorial Q_3 (×), and proximal Q_4 (△) point charges and homogeneous electric field (▲).

stand causes of the origin of the α_δ dispersion, let us consider the effects of these two charges on the state of the coordinated CO. Note, first of all, that in both cases δ is affected by the change in q, whereas ν_{CO} is mainly affected by the back-bonding alteration. Q_1 is located close to the CO oxygen and affects both σ donation and π back-bonding, whereas Q_4 changes mainly back-bonding, hardly affecting the σ donation. Therefore, Q_4 affects δ and ν_{CO} only through the change in the back-bonding, whereas Q_1 affects δ by changing both the σ donation and π back-bonding, with ν_{CO} still being controlled mainly by the back-bonding. Thus α_δ is expected to be larger in the Q_1 case. The homogeneous electric field and Q_3 charges affect the σ donation to the oxygen more than the Q_1 charges and less than the Q_4 charges. Therefore the α_δ values corresponding to these cases have intermediate magnitudes.

Note that the calculated value of $\alpha_\delta = 0.24$ ppm/cm^{-1} corresponding to the homogeneous electric field is about two times smaller than that calculated by Augspurger et al. (1991) for the free carbon monoxide in the field, 0.47 ppm/cm^{-1}. It follows from the previous discussion that, most probably, this deviation is caused by the large effect of the electric field on the back-bonding, which is not taken into account by Augspurger et al. (1991) and very strongly changes ν_{CO} (paper 1).

The only deviation from the discussed linear correlation between $\Delta\delta$ and $\Delta\nu_{CO}$ takes place for the distal Q_2 charges (Fig. 8 *b*). These charges were shown in paper 1 to affect the σ donation and back-bonding in the same direction. For example, a positive charge located at $r = 6$ Å (Fig. 1 *c*) decreases both the σ donation and π back-bonding, the latter being less affected (Fig. 3, *b* and *d*, of paper 1). This EDT increases q and decreases $q(2\pi^*)$. Consequently, the charge under consideration is expected to decrease δ and increase ν_{CO}. These are the Q_2 point charges located in the region of the porphyrin edge that cause a very complicated relationship between δ and ν_{CO} (*empty circles* scattered around the (0,0) point in Fig. 8 *b*).

The correlation between Γ and ν_{CO} is also close to linear (Fig. 8 *a*) in all cases but the Q_2 case,

$$\Delta\Gamma = (5 \div 10)\nu_{CO}\ \text{kHz/cm}^{-1}, \qquad (18)$$

and the highest and lowest values of the slopes of the straight lines describing this correlation, $\alpha_G = 5$ and 10 kHz/cm^{-1}, correspond to the proximal and distal point charges.

In a recent paper Park et al. (1991) presented the available experimental data on δ and Γ of different HP(CO)s and showed that there are linear correlations between δ and Γ on one hand and ν_{CO} on the other. The experimental values of 0.26 ppm/cm^{-1} and 11 kHz/cm^{-1} were obtained for α_δ and α_G, respectively.

These experimental values are very close to the theoretical values obtained for the different cases of electrostatic perturbations considered in this paper. This result favors the conclusion of Oldfield et al. (1991) and Park et al. (1991) that the main mechanism determining the change of the NMR and vibrational characteristics of the CO coordinated by different HPs and their models are electrostatic interactions of the Fe(P)(Im)(CO) unit with the charged or polar protein amino acids.

Effect of the distal histidine electric field on ν_{CO}, δ, and Γ

The theoretical investigation of the effect of the point charges and homogeneous electric field on the electronic structure of Fe(P)(Im)(CO) presented above shows that in principle the protein electric field can essentially contribute to the spectroscopic features of HP(CO)s. In this section the electronic structure of the SWMb(CO) active center and the effect of the electric field of different tautomeric states of the distal histidine and its cation on the Mb(CO) spectroscopic parameters are discussed.

First of all, note that in the x-ray studies of Fe(P)(Im)(CO) and Mb(CO), very different magnitudes of R_{FeC} were obtained: 1.75 and 1.90 Å, respectively. However, very similar ν_{CO} values were observed in the model

compounds and Mb(CO). This observation contradicts our theoretical calculations (paper 1), which showed that in general, a 0.01 Å increase in R_{FeC} increases ν_{CO} by about 5 cm^{-1}, implying that ν_{CO} must strongly depend on R_{FeC}. In particular, the R_{FeC} increase from 1.75 to 1.9 Å was calculated in the present work to increase ν_{CO} from 1978.5 to 2046.2 cm^{-1}. This result brings one to the conclusion that the difference between the R_{FeC} magnitudes in Mb(CO) and model compounds does not exceed several hundredths of an angstrom.

The x-ray studies of relatively small chemical compounds are much more precise than those of proteins, where the R_{FeC} uncertainty is on the order of 0.1–0.2 Å (G. N. Phillips, Jr., private communication). Therefore, our results suggest that the x-ray diffraction studies of Mb(CO) (Quillin et al., 1993) overestimate the iron-carbon distance.

To compare the theoretical and experimental results on the distal histidine electric field effect, the differences in ν_{CO}, δ, and Γ between the cases without and with the distal histidine occupying different conformational substates are addressed in this section.

The special notations for the spectroscopic parameters under consideration in different conformational substates are used hereafter. For example, $\nu_{CO}(A_0)$ corresponds to ν_{CO} of HP(CO) in the A_0 conformational substate, whereas $\Delta\delta(\delta 180, \epsilon 180)$ equals the difference between the ^{17}O isotropic chemical shifts in the presence of $His^{\delta,180}$ and $His^{\epsilon,180}$. Using these notations, for instance, the difference between Γ in the presence of $His^{\epsilon,180}$ and Γ in its absence is denoted by $\Delta\Gamma(\epsilon 180, 0)$.

The sign of the effect of the electric field of different His conformational substates can be predicted qualitatively on the basis of the study of the effect of different distal point charges on ν_{CO}, δ, and Γ. For example, His^+ is positively charged and, consequently, is expected to decrease all of these spectroscopic parameters. Neutral His^{ϵ} can be simulated by a dipole with the positive end located near the CO oxygen, whereas His^{δ} represents the oppositely oriented dipole of approximately the same magnitude. Therefore, His^{ϵ} and His^{δ} electric fields are expected to change ν_{CO}, δ, and Γ in opposite directions by approximately the same values.

The data presented in Table 2 agree with these deductions, the results on the effects of $His^{\delta,180}$ and $His^{\epsilon,180}$ also being qualitatively understood in the same way.

These theoretical results can be used to explain the observation of four C-O vibration absorption bands in the IR spectra of different HP(CO)s. Indeed, the calculations show that the electric field of His^{δ} and $His^{\epsilon,180}$ increases, and that of $His^{\delta,180}$ and His^{ϵ} decreases ν_{CO} with respect to its value in the free heme-(CO), where $\Delta\nu_{CO}(\delta, \epsilon 180)$, $\Delta\nu_{CO}(\epsilon 180, \delta 180)$, $\Delta\nu_{CO}(\delta 180, \epsilon)$ are equal 12.1, 10.4, and 6.7 cm^{-1}, respectively. These values are close to the experimentally observed differences between the positions of the four C-O stretch bands in different HP(CO)s. For example, in SWMb(CO) at pH 7.8 these bands are located at 1966 (A_0), 1952.0 (A_2), 1944.0 (A_1), and 1933.4 (A_3) cm^{-1}; their relative intensities equal 2.5%, 7.2%, 50.7%, and 39.6%, respectively, and the $\Delta\nu_{CO}(A_0, A_2)$, $\Delta\nu_{CO}(A_2, A_1)$, and $\Delta\nu_{CO}(A_1, A_3)$ values equal 14, 8, and 10.6 cm^{-1}, respectively (Potter et al., 1990). This comparison supports the assumption of Oldfield et al. (1991) that the orientation and tautomeric state of the neutral His could be the parameters controlling the positions and relative intensities of these four IR peaks.

However, this interpretation meets at least one very serious problem. Morikis et al. (1989), Ramsden and Spiro (1989), Sage et al. (1991), and Balasubramanian et al. (1993) showed that at low pH ($\leq$5.0), the most absorbance intensity converges to the 1965 cm^{-1} band and assumed that this band corresponds to the protein conformation with the distal histidine displaced out of the heme pocket. This assumption was supported by the result that the IR spectra of the Mb(CO) mutants with the distal histidine substituted for different small nonpolar amino acids contain only one C-O stretch band with the maximum at 1965 cm^{-1} (Morikis et al., 1989; Balasubramanian et al., 1993; Li et al., 1994), and was finally proved by the direct x-ray diffraction studies of SWMb(CO) at pH 4 (Yang and Phillips, 1996). The fact that in the native SWMb(CO) at pH 7.8 $\nu_{CO}(A_0)$ = 1966 cm^{-1} (Potter et al., 1990) implies that at physiological pH the A_0 conformer corresponds to the protein conformation with the distal histidine displaced out of the heme pocket, and the relative intensity of the A_0 band is controlled by the population of this conformational substate.

Because the A_0 conformer corresponds to the highest ν_{CO} value, the experimental data imply that the presence of the distal histidine reduces ν_{CO} with respect to its value in the proteins with the histidine substituted or displaced out of the heme pocket. Because the electric field of both His^{δ} and $His^{\epsilon,180}$ was calculated to increase ν_{CO}, only two $His^{\delta,180}$ and His^{ϵ} conformations can be considered to cause the appearance of the number of the C-O stretch bands in HP(CO)s. Therefore, it follows from our calculations that the His^{δ} and $His^{\epsilon,180}$ conformational substates are very weakly populated, if at all, in HP(CO)s at physiological pH.

It was noted above that the $His^{\delta,180}$ and His^{ϵ} electric fields were calculated to lead to the two C-O bands, with the peak difference of $\Delta\nu_{CO}(\delta 180, \epsilon)$ = 6.7 cm^{-1}, which is very close to the experimentally observed 8 cm^{-1}. However, $\Delta\nu_{CO}(\delta 180, 0) = -6.9$ and $\Delta\nu_{CO}(\epsilon, 0) = -13.6$ cm^{-1} (Table 2); both of these values are about 8 cm^{-1} smaller than the experimentally observed ones (in SWMb(CO) at pH 7.8 $\Delta\nu_{CO}(A_2, A_0) = -14.0$ and $\Delta\nu_{CO}(A_1, A_0) = -22.0$ cm^{-1}). This discrepancy can be attributed to the small (about 0.015 Å; see paper 1) shortening of the Fe-CO bond caused by the steric interaction with the distal histidine in any of the considered conformations.

To compare the theoretical and experimental results on δ, one must take into account that the characteristic time of NMR spectroscopy is about 10^{-5} s, which is much longer than the characteristic times of different protein motions at room temperature, most of which are faster than 10^{-7} s (Parak and Knapp, 1984). Therefore, any NMR spectrum of

HP(CO) is expected to describe the protein system averaged over the populated conformational substates. This conclusion is supported by Park et al. (1991), who showed that the NMR spectra of different HP(CO)s contain only one ^{17}O band.

At low pH the protein occupies only one A_0 conformation. Consequently, δ at low pH corresponds to this A_0 conformation. At physiological pH the system migrates mainly between the A_1 and A_3 conformational substates, the populations of which equal 50.7% and 39.6%, respectively (Potter et al., 1990). Therefore, at physiological pH the observed δ represents the result of the averaging over the values corresponding to these two conformational substates.

Because the A_1 and A_3 substates are almost equally populated in SWMb(CO) at physiological pH, the experimentally observed difference between the observed δ values at pH 5.0 and 7.8 (or between the distal histidine substituted and native Mb(CO)) equals

$$\Delta\delta(\mathrm{pH}) = \delta(A_0) - 1/2[\delta(A_1) + \delta(A_3)] = \Delta\delta(A_0,A_1) + 1/2\Delta\delta(A_1,A_3). \quad (19)$$

It was shown above on the basis of the comparison of the theoretical and experimental results on ν_{CO} that most probably the A_1 conformational substate corresponds to the His^{ϵ} with a R_{FeC} about 0.015 Å shorter than that in the low pH case. Taking into account the effect of this shortening of R_{FeC} and the data presented in Table 2, we obtain $\Delta\delta(A_0, A_1) \approx \Delta\delta(0,\epsilon) + 0.2 = 2.4$ ppm (Table 2).

$\Delta\delta(A_1,A_3)$ can be estimated to equal 1.6 ÷ 5.0 ppm, using the linear correlation between the changes of ν_{CO} and δ (Eq. 17), and the fact that in SWMb(CO) $\Delta\nu_{CO}(A_1, A_3) = 10.6\ cm^{-1}$.

Using these values of $\Delta\delta(A_0, A_1)$ and $\Delta\delta(A_1, A_3)$, we obtain from Eq. 18 $\Delta\delta(\mathrm{pH}) = 3.2 \div 4.9$ ppm; the experimentally observed value of 4.2 ppm (Park et al., 1991) is in this theoretically obtained interval.

Using correlations between $\Delta\Gamma$ and $\Delta\nu_{CO}$ (Eq. 18), the quantum chemically calculated value of $\Delta\Gamma(\epsilon, 0)$ (Table 2), performing the same averaging, and taking into account the dependence of Γ on R_{FeC}, one obtains $\Delta\Gamma(\mathrm{pH}) = 0.14 \div 0.17$ MHz; this value is also close to the experimentally obtained one, 0.25 ± 0.15 MHz (Park et al., 1991).

The formation of the cation of the distal histidine could also strongly affect the spectroscopic parameters under consideration. The electric field of His^+ was calculated to decrease ν_{CO} by 30.1 cm^{-1} (Table 2). Assuming that the steric interaction with the distal histidine cation shortens R_{FeC} by the same 0.015 Å, we obtain $\Delta\nu_{CO}(0, +) = 38\ cm^{-1}$, this value being slightly larger than the experimentally observed $\Delta\nu_{CO}(A_0, A_3) = 32.4\ cm^{-1}$. Assuming that the A_3 conformer corresponds to the heme-CO complex with the Fe-CO distance shortened by 0.015 Å in the presence of the distal His^+ in the heme pocket and using Eq. 19, one obtains $\Delta\delta(\mathrm{pH}) = 4.9$ ppm and $\Delta\Gamma(\mathrm{pH}) = 0.22$ MHz. The former value is also slightly larger than the experimentally observed one, 4.2 ppm, the latter being in the interval of the precision of the experiment, 0.25 ± 0.15 MHz.

Taking into account that the pK value of the free histidine is 7, it could be assumed that an equilibrium His ↔ His^+ takes place in HP(CO)s at physiological pH, and the intensity of the A_3 band provides one with the information about the population of the cationic state of the histidine.

This interpretation, however, contradicts the experimental data (Giacometti et al., 1977; Fuchsman and Appleby, 1979; Traylor et al., 1983; Coletta et al., 1985; Ramsden and Spiro, 1989; Morikis et al., 1989) showing that in the protein the distal histidine has a pK_a of 4.4, and consequently at physiological pH it is expected to be neutral. Moreover, it was noted above that even if the cation has been formed at physiological pH, it would be expected to be displaced out of the heme pocket and exposed to the solvent. Therefore, the possibility of the formation of the distal histidine cation and its presence in the heme pocket at physiological pH do not seem to be well grounded.

Nevertheless, the results on the effect of the His^+ electric field on ν_{CO} allow us to propose another model for the A_3 conformer. Indeed, it follows from our calculations that the cation electric field is expected to reduce ν_{CO} to the values that are smaller than the experimentally observed ones. Therefore, one can assume that the A_3 conformer corresponds to the presence of the distal histidine in some charge state intermediate between His^{ϵ} and His^+. Such a state can be formed by a hydrogen bond between the distal histidine N_δ in HP(CO) and some other amino acid or the solvent water. The latter possibility is supported by the crystal x-ray diffraction studies of Quillin et al. (1993), who showed that in Mb(CO) N_δ is exposed to water, and the closest water molecule oxygen is located 2.87 Å from it (G. Phillips, private communication), this distance being typical for the O-H · · · N hydrogen bond. The effect of the formation of the water-N_δ hydrogen bond on ν_{CO} is now under quantitative theoretical study.

From this point of view the four C-O vibrational bands can be assigned to four different conformations of the distal histidine: His displaced out of the pocket (A_0), His located in the pocket in the $His^{\delta,180}$ (A_2), and His^{ϵ} (A_1) tautomeric forms and His^{ϵ} with N_ϵ hydrogen-bonded to the solvent water (A_3). The relative intensities of each band are controlled by the population of each conformation.

It follows from Table 2 that the presence of the distal histidine in the heme pocket and its motion between the His^{ϵ} and $His^{\delta,180}$ conformational substates essentially affect both the Fe-C and C-O atomic bond indexes. The corresponding three points are presented in Fig. 6 (*open squares*) from which it is simple to see that the correlation between ΔB_{FeC} and B_{CO} is also close to linear and $\alpha_B = -1.4$.

This value is about three times larger than that for the distal point Q_1 or Q_2 charges (paper 1). This result is understandable, because the His electric field is produced by a number of different charges, its gradient is much smaller than that of the one isolated point charge at the distances characteristic for the His-CO distances, and, consequently,

the effect of the change in the His tautomeric state and orientation is closer to the effect of the change in the homogeneous electric field, for which α_B was shown in paper 1 to equal -1.

The theoretical value $\alpha_B = -1.4$ corresponds to $\alpha_\nu = -0.7$, which is close to the experimental one, -0.8 (Ramsden and Spiro, 1989; Morikis et al., 1989; Sage et al., 1991; Zhu et al., 1992; Ling et al., 1994). The weak underestimation of α_ν can be a result of the change of R_{FeC} upon the appearance of His in the heme pocket, which was neglected in these calculations and was shown in paper 1 to increase the α_ν value.

CONCLUSION

In this work the theoretical analysis of the features of C-O and Fe-C chemical bonds and corresponding vibrational frequencies, ^{17}O isotropic chemical shift, and nuclear quadrupole constant of HP(CO)s was continued.

It was shown by using the vibronic theory of activation and quantum chemical calculations that the distortions of the heme complex can explain neither wide variation of ν_{CO}, δ, and Γ in different HP(CO)s, nor their correlation. The electrostatic interactions with the charged or polar groups of the heme environment were shown to be the only interaction that can explain the features of the infrared and nuclear magnetic resonance spectra of these proteins.

It was shown that ν_{CO} mainly provides one with the information on the extent of the back-bonding, δ is proportional to the electron density on the oxygen, and Γ strongly depends on the axial asymmetry of this electron density distribution. The charged groups located on the distal side of the heme affect δ and Γ much more strongly than that located in the proximal and equatorial parts of the heme pocket, whereas ν_{CO} is essentially affected by all of these charges. The latter feature was shown to be a result of the strong delocalization of the axial CO-Fe-Im π electronic subsystem.

Taking into account the effect of the neutral distal histidine electric field and its cation allowed us to interpret the conformational substate of HP(CO)s as the one that differs by His orientation and tautomeric state: A_0 corresponds to His displaced out of the heme pocket; A_2 is the His with a protonated distal nitrogen and rotated by 180° around the C_β-C_γ bond; and A_1 is the His with a protonated proximal nitrogen. The His^δ and $His^{\epsilon,180}$ conformational substates were shown to increase ν_{CO} with respect to its A_0 value. Therefore it was concluded that their population is very low in HP(CO)s.

The A_3 conformational substate could be a state in which a hydrogen bond is formed between the distal histidine and some amino acid or water molecule. It could also correspond to some other metastable orientations of the neutral distal histidine (in addition to the four considered above).

The electrostatic interactions with the proximal or equatorial point charges were shown to essentially contribute to ν_{CO}. This conclusion implies that the changes in the geometry or protonation state of the proximal and equatorial heme environment during the anharmonic protein motion can also lead, in principle, to the presence of the number of the C-O stretch bands in the infrared spectra of HP(CO)s.

To test all of these possibilities, the trajectory of the distal histidine is now being studied with the use of the molecular dynamics simulations, and the combined VTA-QC approach is being used to calculate the effect of this motion on ν_{CO}.

In general, it follows from the results of this paper that the developed theoretical techniques reliably describe the dependence of the protein spectroscopic properties on the magnitude and dynamics of the protein electric field and, therefore, can be used to test different models describing the latter.

We would like to thank Dr. Abel Schejter for helpful discussions.

This work was supported by the Sackler Fund for Scientists Absorption, the Gileadi Program of the Center for Scientists Absorption, Ministry of Absorption of Israel, and grant of Ministry of Science of Israel no. 6531194. This work is in partial fulfillment of the requirements for the Ph.D. degree (BK) from the Sackler School of Medicine at Tel Aviv University.

REFERENCES

Anderson, W. P., W. D. Edwards, and M. C. Zerner. 1986. Calculated spectra of hydrated ions of the first transition-metal series. *Inorg. Chem.* 25:2728–2732.

Augspurger, J. D., C. E. Dykstra, and E. Oldfield. 1991. Correlation of carbon-13 and oxygen-17 chemical shifts and the vibrational frequency of electrically perturbed carbon monoxide: a possible model of distal ligand effects in carbonmonoxyheme proteins. *J. Am. Chem. Soc.* 113: 2447–2451.

Bacon, A. D., and M. C. Zerner. 1979. An intermediate neglect of differential overlap theory for transition metal complexes: Fe, Co and Cu chlorides. *Theor. Chim. Acta.* 53:21–54.

Balasubramanian, S., D. G. Lambright, and S. G. Boxer. 1993. Perturbations of the distal heme pocket in human myoglobin mutants probed by infrared spectroscopy of bound CO: correlation with ligand binding kinetics. *Proc. Natl. Acad. Sci. USA.* 90:4718–4722.

Bersuker, I. B. 1978. Mutual vibronic influence of weakly coordinated molecular systems in chemical reactions and catalysis. *Chem. Phys.* 31:85–93.

Bersuker, I. B. 1984. The Jahn-Teller Effect and Vibronic Interactions in Modern Chemistry. Plenum, New York.

Brantley, R. E., Jr., S. J. Smerdon, A. J. Wilkinson, E. W. Singleton, and J. S. Olson. 1993. The mechanism of autoxidation of myoglobin. *J. Biol. Chem.* 268:6995–7010.

Buchner, W., and W. A. Schenk. 1982. Interpretation of ^{13}C chemical shifts in transition metal carbonyl complexes. *J. Magn. Res.* 48:148–151.

Cameron, A. D., S. J. Smerdon, A. J. Wilkinson, J. Habash, J. R. Helliwell, T. Li, and J. S. Olson. 1993. Distal pocket polarity in ligand binding to myoglobin: deoxy and carbonmonoxy forms of a threonine^{68}(E11) mutant investigated by X-ray crystallography and infrared spectroscopy. *Biochemistry.* 32:13061–13070.

Chipot, C., B. Maigret, J.-L. Rivail, and H. A. Scheraga. 1992. Modelling amino acid side chains. 1. Determination of net atomic charges from ab initio self-consistent field molecular electrostatic properties. *J. Phys. Chem.* 96:10276–10284.

Coletta, M., P. Ascenzi, T. G. Traylor, and M. Brunori. 1985. Kinetics of carbon monoxide binding to monomeric hemoproteins. *J. Biol. Chem.* 260:4151–4155.

Decatur, S. M., and S. G. Boxer. 1995. A test of the role of electrostatic interactions in determining the CO stretch frequency in carbonmonoxymyoglobin. *Biochem. Biophys. Res. Commun.* 212:159–164.

Du, P., F. U. Axe, G. H. Loew, S. Canuto, and M. C. Zerner. 1991. Theoretical study on the electronic spectra of model compound II complexes of peroxidases. *J. Am. Chem. Soc.* 113:8614–8621.

Du, P., and G. H. Loew. 1992. Role of axial ligand in the electronic structure of model compound I complexes. *Int. J. Quant. Chem.* 44: 251–261.

Du, P., and G. H. Loew. 1995. Theoretical study of model compound I complexes of horseradish peroxidase and catalase. *Biophys. J.* 68: 69–80.

Eaton, W. A., L. K. Hanson, P. J. Stephens, J. C. Sutherland, and J. B. R. Dunn. 1978. Optical spectra of oxy- and deoxyhemogloblin. *J. Am. Chem. Soc.* 100:4991–5003.

Edwards, W. D., B. Weiner, and M. C. Zerner. 1986. On the low-lying states and electronic spectroscopy of iron(II) porphine. *J. Am. Chem. Soc.* 108:2196–2204.

Edwards, W. D., B. Weiner, and M. C. Zerner. 1988. Electronic structure and spectra of various spin states of (porphinato)iron(III) chloride. *J. Phys. Chem.* 92:6188–6197.

Eichorn, G. L. 1973. Inorganic Biochemistry. Elsevier, Amsterdam.

Fuchsman, W. H., and C. A. Appleby. 1979. CO and O_2 complexes of soybean leghemoglobins: pH effects upon infrared and visible spectra. Comparisons with CO and O_2 complexes of myoglobin and hemoglobin. *Biochemistry.* 18:1309–1321.

Geissinger, P., B. E. Kohler, and J. C. Woehl. 1995. Electric field and structure in the myoglobin heme pocket. *J. Phys. Chem.* 99: 16527–16529.

Ghosh, A., and D. F. Bocian. 1996. Carbonyl tilting and bending potential energy surface of carbon monoxyhemes. *J. Phys. Chem.* 100: 6363–6367.

Giacometti, G. M., T. G. Traylor, P. Ascenzi, M. Brunori, and E. Antonini. 1977. Reactivity of ferrous myoglobin at low pH. *J. Biol. Chem.* 252: 7447–7448.

Hu, S., K. M. Vogel, and T. G. Spiro. 1994. Deformability of heme protein CO adducts: FT-IR assignment of the FeCO bending mode. *J. Am. Chem. Soc.* 116:11187–11188.

Ivanov, D., J. T. Sage, M. Keim, J. R. Powell, S. A. Asher, and P. M. Champion. 1994. Determination of CO orientation in myoglobin by single-crystal infrared linear dichroism. *J. Am. Chem. Soc.* 116: 4139–4140.

Jameson, C. J. 1994. Theoretical and physical aspects of nuclear shielding. *In* Nuclear Magnetic Resonance, Vol. 23. G. A. Webb, editor.

Jameson, C. J., and H. S. Gutowsky. 1964. Calculation of chemical shifts. I. General formulation and the Z dependence. *J. Chem. Phys.* 40: 1714–1724.

Jewsbury, P., and T. Kitagawa. 1994. The distal residue-CO interaction in carbonmonoxy myoglobins: a molecular dynamics study of two distal histidine monomers. *Biophys. J.* 67:2236–2250.

Jewsbury, P., and T. Kitagawa. 1995. The distal residue-CO interaction in carbonmonoxy myoglobins: a molecular dynamics study of three distal mutants. *Biophys. J.* 68:1283–1294.

Jewsbury, P., S. Yamamoto, T. Minato, M. Saito, and T. Kitagawa. 1995. The proximal residue largely determines the CO distortion in carbon monoxy globin proteins. An *ab initio* study of a heme prosthetic unit. *J. Phys. Chem.* 99:12677–12685.

Karplus, M., and J. A. Pople. 1963. Theory of carbon NMR chemical shifts in conjugated molecules. *J. Chem. Phys.* 38:2803–2807.

Kim, K., J. Fettinger, J. L. Sessler, M. Cyr, J. Hugdahl, J. P. Collman, and J. A. Ibers. 1989. Structural characterization of a sterically encumbered iron(II) porphyrin CO complex. *J. Am. Chem. Soc.* 111:403–405.

Kim, K., and J. A. Ibers. 1991. Structure of a carbon monoxide adduct of a "capped" porphyrin: Fe(C_2-Cap)(CO)(1-methylimidazole). *J. Am. Chem. Soc.* 113:6077–6081.

Kushkuley, B., and S. S. Stavrov. 1996. Theoretical study of the distal-side steric and electrostatic effects on the vibrational characteristics of the FeCO unit of the carbonylheme proteins and their models. *Biophys. J.* 70:1214–1229.

Lee, H. C., M. Ikeda-Saito, T. Yonetani, R. S. Magliozzo, and J. Peisach. 1992. Hydrogen bonding to the bound dioxygen in oxy cobaltous myoglobin reduces the superhyperfine coupling to the proximal histidine. *Biochemistry.* 31:7274–7281.

Lee, H. C., J. Peisach, Y. Dou, and M. Ikeda-Saito. 1994. Electron-nuclear coupling to the proximal histidine in oxy cobalt-substituted distal histidine mutants of human myoglobin. *Biochemistry.* 33:7609–7618.

Lee, H. C., J. Peisach, A. Tsuneshige, and T. Yonetani. 1995. Electron spin echo envelope modulation study of oxygenated iron-cobalt hybrid hemoglobins reveals features analogous to those of the oxy ferrous protein. *Biochemistry.* 34:6883–6891.

Lee, H. C., J. B. Wittenberg, and J. Peisach. 1993. Role of hydrogen bonding to bound dioxygen in soybean leghemoglobin. *Biochemistry.* 32:11500–11506.

Li, T., M. L. Quillin, G. N. Phillips, and J. S. Olson. 1994. Structural determinants of the stretching frequency of CO bound to myoglobin. *Biochemistry.* 33:1433–1446.

Li, X.-Y., and T. G. Spiro. 1988. Is bound CO linear or bend in heme proteins? Evidence from resonance Raman and infrared spectroscopic data. *J. Am. Chem. Soc.* 110:6024–6033.

Lian, T., B. Locke, T. Kitagawa, M. Nagai, and R. M. Hochstrasser. 1993. Determination of the Fe-CO geometry in the subunits of carbonmonoxy hemoglobin M Boston using femtosecond infrared spectroscopy. *Biochemistry.* 32:5809–5814.

Lim, M., T. A. Jackson, and P. A. Anfinrud. 1995. Binding of CO to myoglobin from a heme pocket docking site to form nearly linear Fe-C-O. *Science.* 269:962–966.

Ling, J., T. Li, J. S. Olson, and D. F. Bocian. 1994. Identification of the iron-carbonyl stretch in distal histidine mutants of carbonmonoxymyoglobin. *Biochim. Biophys. Acta.* 1188:417–421.

Loew, G. H. 1983. Theoretical investigations of iron porphyrins. *In* Iron Porphyrins. Part 1. A. B. P. Lever and H. B. Gray, editors. Addison-Wesley, London. 1–87.

London, F. 1937. Théorie quantique des courants interatomiques dans les combinaisons aromatiques. *J. Phys. Radium.* 8:397–409.

Lucken, E. A. C. 1969. Nuclear Quadrupole Coupling Constants. Academic Press, London.

Morikis, D., P. M. Champion, B. A. Springer, and S. G. Sligar. 1989. Resonance Raman investigations of site-directed mutants of myoglobin: effect of distal histidine replacement. *Biochemistry.* 28:4791–4800.

Oldfield, E., K. Guo, J. D. Augspurger, and C. E. Dykstra. 1991. A molecular model for the major conformational substates in heme proteins. *J. Am. Chem. Soc.* 113:7537–7541.

Parak, F., and E. W. Knapp. 1984. A consistent picture of protein dynamics. *Proc. Natl. Acad. Sci. USA.* 81:7088–7092.

Park, K. D., K. Guo, F. Adebodun, M. L. Chiu, S. G. Sligar, and E. Oldfield. 1991. Distal and proximal ligand interactions in heme proteins: correlations between C-O and Fe-C vibrational frequencies, oxygen-17 and carbon-13 nuclear magnetic resonance. *Biochemistry.* 30: 2333–2347.

Poole, C. P., Jr., and H. A. Farach. 1972. The Theory of Magnetic Resonance. Wiley-Interscience, New York.

Pople, J. A. 1962. Molecular-orbital theory of diamagnetism. I. An approximate LCAO scheme. *J. Chem. Phys.* 37:53–59.

Potter, W. T., J. H. Hazzard, M. G. Choc, M. P. Tucker, and W. S. Caughey. 1990. Infrared spectra of carbonyl hemoglobins: characterization of dynamic heme pocket conformers. *Biochemistry.* 29:6283–6295.

Quillin, M. L., R. M. Arduini, J. S. Olson, and G. N. Phillips, Jr. 1993. High-resolution crystal structures of distal histidine mutants of sperm whale myoglobin. *J. Mol. Biol.* 234:140–155.

Quillin, M. L., T. Li, J. S. Olson, G. N. Phillips, Jr., Y. Dou, M. Ikeda-Saito, R. Regan, M. Carlson, Q. H. Gibson, H. Li, and R. Elber. 1995. Structural and functional effects of apolar mutations of the distal valine in myoglobin. *J. Mol. Biol.* 245:416–436.

Ramsden, J., and T. G. Spiro. 1989. Resonance Raman evidence that distal histidine protonation removes the steric hindrance to upright binding of carbon monoxide by myoglobin. *Biochemistry.* 28:3125–3128.

Ray, G. B., X.-Y. Li, J. A. Ibers, J. L. Sessler, and T. G. Spiro. 1994. How far can proteins bend the FeCO unit? Distal polar and steric effects in heme proteins and models. *J. Am. Chem. Soc.* 116:162–176.

Ricard, L., R. Weiss, and M. Momenteau. 1986. Crystal and molecular structure of a highly hindered iron(II) porphyrin complex. *J. C. S. Chem. Commun.* 818–820.

Ridley, J., and M. Zerner. 1973. An intermediate neglect of differential overlap technique for spectroscopy: pyrrole and the azines. *Theor. Chim. Acta.* 32:111–134.

Sage, J. T., D. Morikis, and P. M. Champion. 1991. Spectroscopic studies of myoglobin at low pH: heme structure and ligation. *Biochemistry.* 30:1227–1237.

Sakan, Y., T. Ogura, T. Kitagawa, F. A. Frauenfelder, R. Mattera, and M. Ikeda-Saito. 1993. Time-resolved resonance Raman study on the binding of carbon monoxide to recombinant human myoglobin and its distal histidine mutants. *Biochemistry.* 32:5815–5824.

Semin, G. K., T. A. Babushkina, and G. G. Yakobson. 1975. Nuclear Quadrupole Resonance in Chemistry. Wiley, New York.

Slater, J. C. 1930. Atomic shielding constants. *Phys. Rev.* 36:57–64.

Springer, B. A., S. G. Sligar, J. S. Olson, and G. N. Phillips, Jr. 1994. Mechanism of ligand recognition in myoglobin. *Chem. Rev.* 94:699–714.

Stavrov, S. S., I. P. Decusar, and I. B. Bersuker. 1993. Chemical activation of oxygen and carbon monoxide by hemoproteins: the vibronic approach. *N. J. Chem.* 17:71–76.

Tetreau, C., D. Lavalette, M. Momenteau, J. Fischer, and R. Weiss. 1994. Structure-reactivity relationship in oxygen and carbon monoxide binding with some heme models. *J. Am. Chem. Soc.* 116: 11840–11848.

Traylor, T. G., L. A. Deardurff, P. Ascenzi, E. Antonini, and M. Brunori. 1983. Reactivity of ferrous heme proteins at low pH. *J. Biol. Chem.* 258:12147–12148.

Ullrich, V. 1979. Cytochrome P450 and biological hydroxylation reactions *Top. Curr. Chem.* 83:67–104.

Yang, F., and G. N. Phillips, Jr. 1996. Crystal structure of CO-, deoxy- and met-myoglobins at various pH values. *J. Mol. Biol.* 256:762–774.

Zerner, M. C., G. H. Loew, R. E. Kirchner, and U. T. Mueller-Westerhoff. 1980. An intermediate neglect of differential overlap technique for spectroscopy of transition-metal complexes. Ferrocene. *J. Am. Chem. Soc.* 102:589–599.

Zhu, L., J. T. Sage, A. A. Rigos, D. Morikis, and P. M. Champion. 1992. Conformational interconversion in protein crystals. *J. Mol. Biol.* 224: 207–215.